



Continuum approach to the quadratic chain: Exact closed-form classification of extended states

D. S. Citrin 

School of Electrical and Computer Engineering, Georgia Institute of Technology, Atlanta, Georgia 30332-0250, USA
and Georgia Tech-CNRS IRL2958, Georgia Tech-Europe, 2 Rue Marconi, 57070 Metz, France

 (Received 24 March 2023; accepted 13 June 2023; published 26 June 2023)

The quadratic chain is a 1D nonperiodic lattice with lattice sites at $z_j = j^2d$ with $j \in \mathbb{W}$ and d the underlying lattice constant. We treat the electronic structure of the quadratic chain in a continuum model. The electronic extended-state spectrum is singular-continuous with bands at wavevectors k rational multiples of $\frac{\pi}{d}$ with critical states occurring at the transitions between extended and localized states as the potential parameter is varied for fixed k . Our treatment results in the exact classification of extended states and provides closed-form expressions to compute them. We further identify states at well-defined energy that are extended for small values of the potential parameter, become localized at higher values, and at yet higher ranges of the parameter, are again extended, dubbing such behavior *reëntrant extended states*.

DOI: [10.1103/PhysRevB.107.235144](https://doi.org/10.1103/PhysRevB.107.235144)

I. INTRODUCTION

Deterministic nonperiodic lattices exhibit properties distinct from those of periodic and random lattices [1–4]. The quadratic chain (QC) is a 1D nonperiodic lattice with lattice sites at $z_j = j^2d$ with $j \in \mathbb{W}$ and d the underlying lattice constant. Recently we showed that the structure factor is singular-continuous and, in a nearest-neighbor tight-binding model, that the spectrum of extended electronic states in the QC exhibits a hierarchy of minibands and minigaps [5]. A similar class of nonperiodic lattices has been studied recently in Ref. [6], and a related photonic structure was studied numerically in Ref. [7]. Here we treat the electronic structure using a continuum approach based on a Kronig-Penney model with δ -function potentials, and show that the hierarchy of bands and gaps found based on numerics in the nearest-neighbor tight-binding model just mentioned are preserved, and, moreover, fully and analytically quantify the extended states in the limit the QC length goes to infinity [cf. Eq. (10)]. The classification of extended states is parallel to the behavior of the peaks in the structure factor [5]. While the tight-binding model can be derived from a continuum approach [8], there are subtle differences [9]. The classification of the extended states has not yet been carried out for the tight-binding approach [5]. In addition, our results here elucidate effects in the QC such as the existence of certain states that remain extended at all values of the potential parameter λ , states that are extended below a state-dependent critical value of the potential parameter, as other states that are extended in disjoint ranges of the potential parameter, calling these latter *reëntrant extended states* [10]. That many of the central properties of QCs appear in both the nearest-neighbor tight-binding model and the Kronig-Penney model is not surprising, but also not a foregone conclusion. Certainly, the two approaches give different numerical predictions. Moreover, we have been successful in exactly computing the states based on the Kronig-Penney model, but not the nearest-neighbor tight-binding model, although the tight-binding model has

yielded a number of analytic results [5]. We further note the number-theoretic aspect of the QC in that we can classify states according to their wavevector k between scattering sites, viz., k that are extended states are rational multiples of $\frac{\pi}{d}$ (but not necessarily the converse).

II. THEORY

In this section we formulate the Kronig-Penney model for the QC from which we derive the transfer matrix. The effective-mass Hamiltonian for an electron is

$$H = -\frac{\hbar^2}{2m^*} \frac{\partial^2}{\partial z^2} + \frac{\hbar^2}{2m^*} \frac{\lambda}{d} \sum_{j=0}^N \delta(z - z_j) \left(1 - \frac{1}{2} \delta_{j,0}\right) \quad (1)$$

with m^* the effective mass and λ characterizing the potential strength. Lattice site $j = 0$ is given half the weight so that the Fourier transform of the potential is proportional to the Jacobi theta function [5, 11]. To simplify the notation, it will be convenient to define the normalized Hamiltonian $\bar{H} = \frac{2m^*}{\hbar^2} H$ and solve the rescaled time-independent Schrödinger equation $\bar{H}\psi = \bar{E}\psi$ where \bar{E} is an eigenvalue of \bar{H} and ψ the corresponding eigenfunction.

Our aim is to compute the extended-state spectrum of the QC. We seek states with \bar{E} connected with $k = \sqrt{\bar{E}}$ between

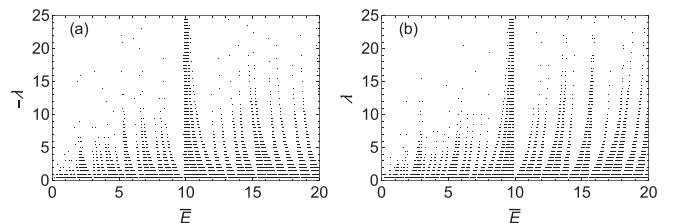


FIG. 1. Energies \bar{E} of extended states in the QC for various λ (a) < 0 , (b) > 0 with $N = 5$

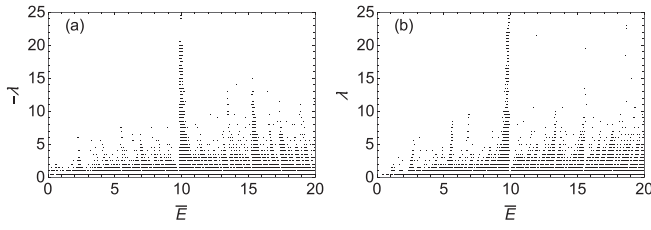


FIG. 2. Energies \bar{E} of extended states in the QC for various λ (a) < 0 , (b) > 0 with $N = 10$.

sites j and $j + 1$ propagating through the QC without attenuation. We adopt a transfer-matrix approach [8]. Focus on the wavefunction near site z_j for some j . For $z_{j-1} < z < z_j$, write $\psi(z) = A_j e^{-ikz} + B_j e^{ikz}$ with A_j and B_j coefficients to be determined. Imposing continuity on ψ and then integrating the Schrödinger equation from $z_j - \epsilon$ to $z_j + \epsilon$ in the limit $\epsilon \rightarrow 0$, we obtain

$$A_{j+1} e^{-ikz_j} + B_{j+1} e^{ikz_j} = A_j e^{-ikz_j} + B_j e^{ikz_j}, \quad (2a)$$

$$A_{j+1} e^{-ikz_j} - B_{j+1} e^{ikz_j} = \left(-\frac{\lambda}{ikd} + 1 \right) A_j e^{-ikz_j} + \left(-\frac{\lambda}{ikd} - 1 \right) B_j e^{ikz_j}. \quad (2b)$$

Writing this in matrix form, we have

$$\begin{bmatrix} A_{j+1} \\ B_{j+1} \end{bmatrix} = M \begin{bmatrix} A_j \\ B_j \end{bmatrix} \quad (3)$$

with

$$M = \begin{bmatrix} 1 + i\gamma & i\gamma \\ -i\gamma & 1 - i\gamma \end{bmatrix}, \quad M_0 = \begin{bmatrix} 1 + i\gamma/2 & i\gamma/2 \\ -i\gamma/2 & 1 - i\gamma/2 \end{bmatrix}, \quad (4)$$

the transfer matrix across quadratic site $j \in \mathbb{N}$ and $j = 0$, respectively, with $\gamma = \frac{\lambda}{2kd}$. The transfer matrix between quadratic sites z_j and z_{j+1} is

$$Q_j = \begin{bmatrix} \exp[-ik(z_{j+1} - z_j)] & 0 \\ 0 & \exp[ik(z_{j+1} - z_j)] \end{bmatrix}. \quad (5)$$

The transfer matrix for a QC with N quadratic sites is

$$T = MQ_{N-1}MQ_{N-2}M \cdots MQ_1MQ_0M_0. \quad (6)$$

Note that the determinant of each transfer matrix is 1. Thus, the eigenvalues ξ_{\pm} of T for a given \bar{E} satisfy $\xi_+ \xi_- = 1$. Extended states then correspond to values of \bar{E} such that $|\xi_+| = |\xi_-| = 1$, or more conveniently, such that $\frac{1}{2} |\text{Tr } T| \leq 1$. Our strategy is

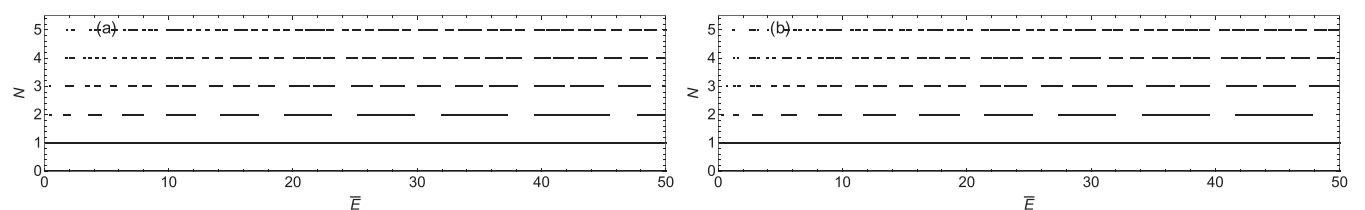


FIG. 3. Energies \bar{E} of extended states in the QC for various N for (a) $\lambda = -3$, (b) 3 with $d = 1$.

thus to find the values of \bar{E} , and hence of k , such that the eigenvalues of Q have unit modulus.

III. NUMERICAL RESULTS

In this section we compute numerically the extended-state spectrum of chains based on Eq. (6). Going forward, without loss of generality we take $d = 1$. Figure 1 shows \bar{E} for extended states with $N = 5$ for various (a) negative and (b) positive λ . Note significant band and gap structures with the bands narrowing and gaps opening with increasing $|\lambda|$ giving the observed structure known as *stacks*. Figure 2 plots \bar{E} of T for $N = 10$. Many of the remarks made above about the case for $N = 5$ apply here as well, although the effects are less marked. λ has a weaker effect on the bands and gaps compared with what is observed in Fig. 1. Stack structures for Fibonacci lattices and for a nonperiodic alloy can be found in Refs. [12,13]. The stack at $\bar{E} = \pi^2$, however, is a characteristic feature that persists to high $|\lambda|$; this stack corresponds to $k = \frac{\pi}{d}$, as will be discussed below where from Eq. (10) will be seen to be associated with an extended state that exists for all values of λ . In Figs. 1 and 2(a) [2(b)] the low (high)-energy side of this stack does not depend on λ . This we shall see is a characteristic of bands in periodic lattices and follows from well-known behavior of the bands found in the Kronig-Penney model with Dirac δ -function potentials. Both edges of the other stacks, however, do shift with λ .

Figure 3 shows the evolution of the bands and gaps for (a) $\lambda = -3$ and (b) 3 for various N . We see the self-similar structure. Bands at N appear to break up into two bands separated by gaps at $N + 1$; new bands arise as well. For example, in Fig. 3(a), the bands at $N = 2$ give rise to two bands each at $N = 3$, but there are also new bands that appear at $N = 3$, e.g., near $\bar{E} = 6, 18, 31$, and 47 . Some gaps persist as N increases (stable gaps) while others close (transient gaps) as an additional band appears, similar to what is observed in a Fibonacci chain [14]. These features merit systematic study.

The QC modulation is now studied between its neighboring cases $z_j = jd$ and $z_j = j^3d$. Figures 4(a) and 4(b) show \bar{E} for $z_j = jd$ with $N = 10$. Note that the horizontal scale is different from that in Figs. 1 and 2. The observed behavior is that of the well-known Kronig-Penney model with Dirac δ -function potentials. Each stack corresponds to a band, and the minigaps within each band are due to the finite chain length N . The stack structure shows widening gaps between bands as $|\lambda|$ increases. On the other hand, in Figs. 5(a) and 5(b) are shown \bar{E} for $z_j = j^3d$ with $N = 10$. Here the stacks are relatively poorly defined for the most part and for a given λ the extended states are fall off quickly with $|\lambda|$. We return to this point below.

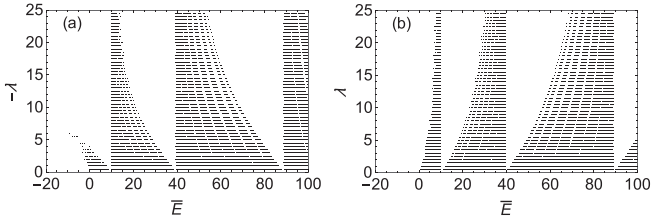


FIG. 4. Energies \bar{E} of extended states in the periodic lattice with $z_j = jd$ for various λ (a) < 0 , (b) > 0 with $N = 10$.

IV. EXACT CLASSIFICATION OF EXTENDED STATES

As we show in this section, the extended states can be fully classified in the $N \rightarrow \infty$ limit in closed form. That is, we will derive in Eq. (10) polynomial inequalities that will yield the ranges of λ for which the states are extended for a given k . Let us consider states with $kd = \pi \frac{r}{s}$ with $r, s \in \mathbb{N}$ coprime. In discussing the extended states in the QC, the termination of the chain at z_0 should not affect the nature of the states. Thus, instead of T , consider the transfer matrix

$$R = mq^{2N}mq^{2(N-1)}mq^{2(N-2)} \dots q^8mq^6mq^4mq^2m \quad (7)$$

where q is a diagonal matrix with respective diagonal elements $e^{\mp ikd}$ and $m = q^{1/2}Mq^{1/2}$. Note that $T = RqM_0$. There are N matrices m in the product in Eq. (7). Consider the factors q^{2j} . It is easy to show $q^{2(j+s)} = q^{2j}$, so that for $kd = \pi \frac{r}{s}$, R is made up of periodic repetitions of the matrix product

$$v = mq^{2(s-1)}mq^{2(s-2)}m \dots mq^4mq^2m \quad (8)$$

where we assume that $N \gg s$. Thus, for a given r and s , the state will be extended provided $\frac{1}{2}|\text{Tr } v| \leq 1$ inasmuch as m and q are unimodular. Now, the trace is preserved by cyclic permutations of the matrix product. Thus, $\frac{1}{2}|\text{Tr } v| = \frac{1}{2}|\text{Tr } v'|$ where

$$v' = q^{s-1}mq^{2(s-2)}m \dots mq^4mq^2mmq^{s-1}. \quad (9)$$

We can simplify v' via the following decimation scheme in the spirit of a real-space renormalization-group approach. Let $m^{(0)} = m$ and $\tilde{m}^{(0)} = m$. Then repeated application of $m^{(j)} = qm^{(j-1)}q$ and $\tilde{m}^{(j)} = qm^{(j-1)}\tilde{m}^{(j-1)}q$ results in $v' = \tilde{m}^{(s-1)}$ with initial conditions $m^{(0)} = m$ and $\tilde{m}^{(0)} = m$. The following cases are exhaustive and classify the extended states: s odd, $\frac{s}{2}$

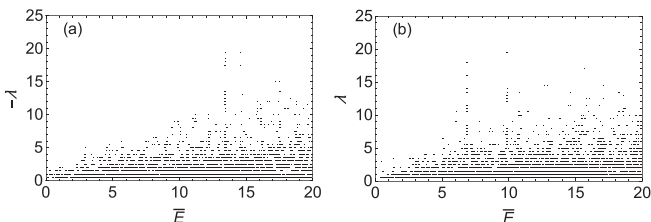


FIG. 5. Energies \bar{E} of extended states in the nonperiodic lattice with $z_j = j^3d$ for various λ (a) < 0 , (b) > 0 with $N = 10$.

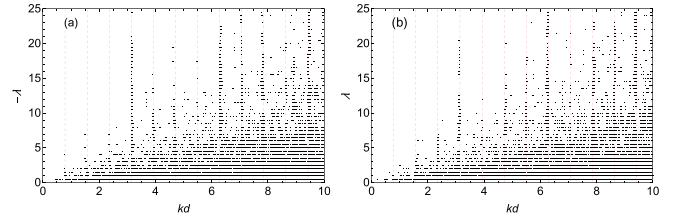


FIG. 6. $kd = \sqrt{\bar{E}}$ of extended states in the QC for various λ (a) < 0 , (b) > 0 with $N = 10$. The data are identical with those for Fig. 2 but rescaling the horizontal axis. Vertical orange dashed lines indicate as a guide to the eye kd integer multiples of $\frac{\pi}{4}$.

even, and $\frac{s}{2}$ odd. We evaluate $\frac{1}{2}|\text{Tr } v'|$ symbolically to give

$$\frac{1}{2}|\text{Tr } v'| = \begin{cases} \left| \sum_{h=0}^{(s-1)/2} (-1)^h \binom{s}{2h} \gamma^{2h} \right|, & s \text{ odd,} \\ \left| 1 + 2\gamma^2 \left[\sum_{h=1}^{s/4} (-1)^h \binom{s/2}{2h} \gamma^{2h-2} \right] \right. \\ \quad \left. \times \left[2 + \sum_{h=1}^{s/4} (-1)^h \binom{s/2}{2h} \gamma^{2h} \right] \right|, & \frac{s}{2} \text{ even,} \\ \left| 1 - 2\gamma^2 \left[\sum_{h=0}^{(s/2-1)/2} (-1)^h \binom{s/2}{2h+1} \gamma^{2h} \right]^2 \right|, & \frac{s}{2} \text{ odd.} \end{cases} \quad (10)$$

Equation (10) is a central result of this paper.

Extended states correspond to solutions for which $\frac{1}{2}|\text{Tr } v'| < 1$ [15]. The expressions in the absolute-value signs are polynomials in γ of degree $s-1$, s , and s . The first few cases give extended states for $s=1$, all λ ; $s=2$, $\gamma^2 \leq 1$; $s=3$, $\gamma^2 \leq \frac{2}{3}$; $s=4$, $\gamma^2 \leq 2$. Thus, apart from the special case $s=1$ for which all $k = \frac{\pi r}{d s}$ with $r, s \in \mathbb{N}$ coprime are extended for all λ , extended states exist only for well-defined ranges of $|\lambda|$ beyond which states are localized. But other interesting effects are observed. Consider, for example, $s=5$. In this case, the values of $|\lambda|$ for which extended states exist is $\gamma^2 \in [0, 1 - \frac{\sqrt{15}}{5}] \cup [1 - \frac{\sqrt{15}}{5}, 2]$. This means, surprisingly, that converting to ranges of $|\lambda|$ for which extended states exist, there are two disjoint ranges. In other words, for a small range of $|\lambda|/(2kd)$ from 0 up to and including $(1 - \frac{\sqrt{15}}{5})^{1/2}$ extended states exist, between $(1 - \frac{\sqrt{15}}{5})^{1/2}$ and $(1 + \frac{\sqrt{15}}{5})^{1/2}$ the states are localized, for $\frac{|\lambda|}{2kd}$ from 2 to $(1 + \frac{\sqrt{15}}{5})^{1/2}$ the states are again extended, while for $\frac{|\lambda|}{2kd} > 2$ the states are all localized. This type of effect also exists for $s \geq 5$. We call this phenomenon *reentrant extended states*. Reentrance has been observed in Refs. [12] and [13] for different types of nonperiodic chains at fixed \bar{E} , but not for an entire stack. We illustrate this effect below in Fig. 7.

Figure 6 replots the data from Fig. 2 on an extended horizontal scale, converting \bar{E} to kd by $kd = \sqrt{\bar{E}}$. Included in the plot are vertical dotted bars showing values of kd that are integer multiples of $\frac{\pi}{4}$. For $kd = \pi, 2\pi$, and 3π ($s=1$), we see particularly well defined stacks, i.e., that the extended states persist up to high values of $|\lambda|$ as predicted above. Figure 6 is in broad agreement with the predictions above; however, unfortunately the numerics are not sufficiently stable in Fig. 6 to clearly see the behavior at all fixed kd as a function of λ . Note, moreover, that these numerical results are for finite N .

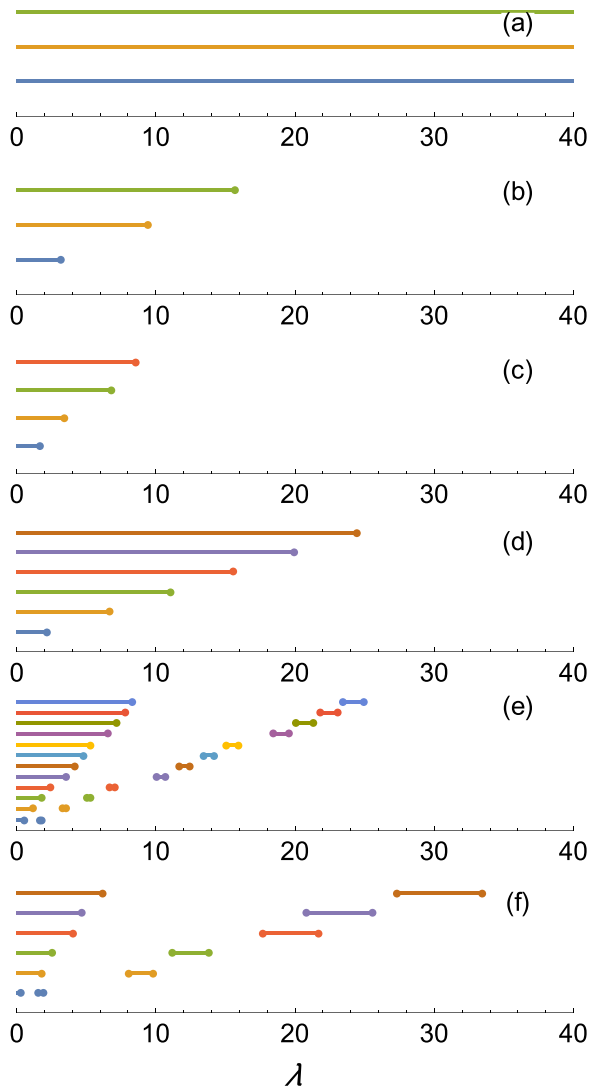


FIG. 7. Extended states as a function of λ for selected values of $kd \leq \pi$. Curves in panels (labeled from bottom to top in each panel) (a) $s = 1$: $kd = \pi, 2\pi, 3\pi$; (b) $s = 2$: $kd = \frac{\pi}{2}, \frac{3\pi}{2}, \frac{5\pi}{2}$; (c) $s = 3$: $kd = \frac{\pi}{3}, \frac{2\pi}{3}, \frac{4\pi}{3}, \frac{5\pi}{3}$; (d) $s = 4$: $kd = \frac{\pi}{4}, \frac{3\pi}{4}, \frac{5\pi}{4}, \frac{7\pi}{4}, \frac{9\pi}{4}, \frac{11\pi}{4}$; (e) $s = 5$: $kd = \frac{\pi}{5}, \frac{2\pi}{5}, \frac{3\pi}{5}, \frac{4\pi}{5}, \frac{6\pi}{5}, \frac{7\pi}{5}, \frac{8\pi}{5}, \frac{9\pi}{5}, \frac{11\pi}{5}, \frac{12\pi}{5}, \frac{13\pi}{5}, \frac{14\pi}{5}$; (f) $s = 6$: $kd = \frac{\pi}{6}, \frac{5\pi}{6}, \frac{7\pi}{6}, \frac{11\pi}{6}, \frac{13\pi}{6}, \frac{17\pi}{6}$.

The ranges of λ over which a given k state is extended are better shown using Eq. (10). Figure 7 shows the range of λ for extended states corresponding to various $kd \leq 3\pi$ for

several values of s . In Fig. 7(a) for kd an integer multiple of π , we see extended states for all λ as noted above. In all other cases, there is a maximum $|\lambda|$ beyond which the k state is localized. Interestingly, for $s \geq 5$, as expected we see reëntrant regions of extended states following an intermediate regime of localized states. This is a general feature of $s \geq 5$.

What about $z_j = j^3 d$? For $z_j = j^n d$ with $n \in \mathbb{N}$, an analysis like that here can be carried out. As n increases, the polynomial equations governing the λ cutoffs are of increasingly high degree, and the extended-state regions thus will be expected to be increasingly fragmented with more complex reëntrant behavior occurring at lower s than for $n = 2$. (Numerically, we find reëntrant behavior for $s \geq 3$.) In addition, to approximate the $N \rightarrow \infty$ limit, much longer QCs are required. It is possible that a classification of extended states is possible based on cubic (or higher-order) Gauss sums [16]; however, there are few results available [17].

V. CONCLUSIONS

In conclusion, we present results for extended states in QCs and classify these states in the limit of long chains. A key result of this paper, therefore, is Eq. (10). Extended states exist below a state-dependent cutoff in $|\lambda|$ for $s > 1$ and these states are characterized by wavevector k between scattering sites where $kd = \pi \frac{r}{s}$ with $r, s \in \mathbb{N}$ coprime. For $s = 1$, states are extended for all $|\lambda|$; for $s \geq 5$ we find reëntrant extended states, i.e., disjoint intervals of $|\lambda|$ in which the states are extended separated by intervals where the states are localized. From a Landauer conductance point of view, if one could isolate individual states, one might be able to observe reëntrant behavior. The importance of reëntrance when many states contribute to the transport, such as might be connected to reëntrant phase transitions [18], quantum diffusion, or the resistivity of a metallic QC, remains to be studied. From a broader perspective, chains with $z_j = j^n d$ are of number-theoretic interest [5]. The extended-state wavevectors k are given by rational multiples of $\frac{\pi}{d}$, the structure factor can be expressed in terms of Gauss sums [16], and for $n = 2$ the structure factor is simply related to the Jacobi theta function [19]. Thus, QCs may enable one type of physical realization of structures directly related to these number-theoretic topics.

ACKNOWLEDGMENT

D.S.C. gratefully acknowledges the support of Conseil Régional Grand Est.

[1] R. Merlin, *IEEE J. Quantum Electron.* **24**, 1791 (1988).
 [2] H. Hiramoto and M. Kohmoto, *Int. J. Mod. Phys. B* **06**, 281 (1992).
 [3] J. B. Sokoloff, *Phys. Rep.* **126**, 189 (1985).
 [4] A. Jagannathan, *Rev. Mod. Phys.* **93**, 045001 (2021).
 [5] D. S. Citrin, *Phys. Rev. B* **107**, 125150 (2023).
 [6] L. Gong, [arXiv:2305.17904v1](https://arxiv.org/abs/2305.17904).
 [7] D. A. Bykov, E. A. Bezus, A. A. Morozov, V. V. Podlipnov, and L. L. Doskolovich, *Phys. Rev. A* **106**, 053524 (2022).
 [8] M. Kohmoto, *Phys. Rev. B* **34**, 5043 (1986).

[9] B. Sutherland and M. Kohmoto, *Phys. Rev. B* **36**, 5877 (1987).
 [10] We also find a small number of critical states at boundaries between extended states and localized states at fixed energy as the potential parameter λ is varied.
 [11] For $z_j = j^2 d$, $\sum_{j=0}^N \delta(z - z_j)(1 - \frac{1}{2}\delta_{j,0}) = \frac{1}{2} \sum_{j=-N}^N \delta(z - z_j)$ accounting for the $1 - \frac{1}{2}\delta_{j,0}$ in the summation in Eq. (1).
 [12] P. Villaseñor-González, F. Mejía, and J. L. Morán-López, *Solid State Commun.* **66**, 1127 (1988).
 [13] T. Nagatani, *Phys. Rev. B* **30**, 6241 (1984); **32**, 2049 (1985).
 [14] F. Piéchon, M. Benakli, and A. Jagannathan, *Phys. Rev. Lett.* **74**, 5248 (1995).

- [15] Critical states correspond to $\frac{1}{2}|\text{Tr}v'| = 1$; the distinction between critical and extended states will be dealt with elsewhere. For our purposes here, *extended states* refers to states that are not localized.
- [16] B. C. Berndt, R. J. Evans, and K. S. Williams, *Gauss and Jacobi Sums* (Wiley, New York, 1998).
- [17] H. Hasse, *Vorlesungen über Zahlentheorie* (Springer-Verlag, Berlin, 1964), pp. 478–489; B. S. Andereck and E. Abrahams, *Physics in One Dimension*, edited by J. Bernasconi and T. Schneider (Springer-Verlag, New York, 1981), pp. 317–320.
- [18] T. Z. Ward, S. Liang, K. Fuchigami, L. F. Yin, E. Dagotto, E. W. Plummer, and J. Shen, *Phys. Rev. Lett.* **100**, 247204 (2008); Y. Tokura, H. Kuwahara, Y. Moritomo, Y. Tomioka, and A. Asamitsu, *ibid.* **76**, 3184 (1996).
- [19] C. G. J. Jacobi, Über die Kreisteilung und ihre Anwendung auf die Zahlentheorie, Bericht Ak. Wiss. Berlin 127 (1837).